Physica B 172 (1991) 143–153
North-Holland

A self-consistent surface-Green-function (SSGF) method

M. Scheffler, Ch. Droste[1], A. Fleszar[2], F. Máca[3], G. Wachutka[4] and G. Barzel
Fritz-Haber-Institut der MPG, Faradayweg 4-6, W-1000 Berlin 33, Germany

We describe the basic aspects of a new, self-consistent Green-function method which allows to calculate the density of states, electron density, and related quantities for a localized perturbation (e.g. an isolated adsorbate or an intrinsic surface defect) at a crystal surface. The method is based on the density-functional theory and combines several ideas from recent theoretical developments, as, for example, from the layer-KKR Green-function method, from ab-initio pseudopotential theory, and from the self-consistent defect-Green-function method. Two applications of the method are presented (S on Pd(1 0 0) and Na on Al(1 0 0)) in order to demonstrate its efficiency and to address a recent controversial discussion concerning the nature of the bonding of alkali adsorbates on metals at very low coverage ($\Theta \to 0$).

1. Introduction

It is well accepted by now that the density-functional theory (DFT) together with the local-density approximation (LDA) for the exchange-correlation functional [1] gives a reliable description of the electron density and of structural and elastic properties of poly-atomic systems (see, e.g., refs. [2, 3] and references therein). Standard DFT-LDA theory transforms the interacting many-electron problem into a self-consistent treatment of non-interacting quasi-particles moving in an effective potential. Whereas perfect crystals are nowadays tractable with high numerical accuracy, it is still a significant challenge to deal with low symmetry poly-atomic systems, as, for example, a surface where Bloch's theorem does not hold and where localized as well as delocalized electronic states are important.

[1] Permanent address: Vereinigte Aluminiumwerke, Georg-von-Boeselager-Str. 25, W-5300 Bonn, Germany.
[2] Permanent address: Physikalisches Institut, Universität Würzburg, Am Hubland, W-8700 Würzburg, Germany.
[3] Permanent address: Institute of Physics, Czechoslovak Academy of Sciences, Na Slovance 2, 180 40 Praha 8, ČSFR.
[4] Permanent address: Institut für Quantenelektronik, Laboratorium für Physikalische Elektronik, ETH-Hönggerberg, HPT, CH-8093 Zürich, Switzerland.

Over the last years and still today several theoretical methods and techniques are being developed for the self-consistent calculation of the surface electronic structure. Grossly speaking we may distinguish (a) cluster methods, (b) super-cell methods, and (c) Green-function methods. All these methods could be divided further into techniques which differ, with respect to their basis set as for example Gaussians, or muffin-tin orbitals, or plane-waves. We will not enter a discussion of these details here.

The first two methods ((a) and (b)) have in common that they are wave function methods, because they require to evaluate many (in principle $\sim 10^{23}$) individual wave functions which are usually far extending and are significantly affected by boundary conditions. In particular cluster methods suffer from this aspect because the majority of the atoms in a cluster is located at the cluster surface giving them an incorrect coordination, electronic structure and electrostatic potential. This problem is significantly reduced in the super-cell or slab approach which may be viewed as a periodically repeated cluster. A remaining problem with super-cells is the interaction of the two surfaces through the slab, which usually has a thickness between four and twelve atomic layers. Theoretical and experimental results indicate that for many surface

properties a system consisting of only a few layers is sufficient (see for example refs. [4, 5]). Super-cell calculations are usually performed for clean surfaces or for high-coverage periodic adlayers. The description of low-coverage systems may be approximately dealt with by using large adlayer unit cells.

For semiconductor surfaces the super-cell approach together with ab-initio pseudopotentials was most successful (see for example ref. [2] and references therein). For general applications and in particular for transition-metal surfaces the super-cell approach together with the full-potential linearized augmented plane-waves method (FLAPW) of Freeman et al. [6, 7] is the most accurate method. Since nearly ten years it represents a standard for any new development. Concerning such new and promising developments we like to mention the full-potential linearized muffin-tin orbitals method (FP-LMTO) of Methfessel and Andersen (see the contribution of Methfessel and Scheffler in these Proceedings, and references therein).

The third class of methods mentioned above (i.e. Green functions) represents the recent developments to treat semi-infinite crystal surfaces. Krüger and Pollmann [8, 9] developed a method to deal with periodic semiconductor surfaces and Inglesfield et al. [10–12] designed a method which is suited for metals. The important low-coverage limit where only one adsorbate particle interacts with a surface, became tractable so far only by the matrix-Green-function method [13] of Feibelman [14, 15]. However, Feibelman has not yet treated semi-infinite crystals, but only very thin slabs of 2–5 layers slabs. Below, we describe a new and different approach which was developed in our group. The principle difference with Feibelman's method is that our approach is a Green-function operator approach and treats a truly semi-infinite system. At this point, it is not clear which of these two methods is the better one. As these methods exist now, both have advantages and disadvantages. We favor our approach but will also describe its shortcomings. Some of them may be corrected in the future.

In short and very simplified, our method may be described as a successor of the self-consistent "defect-Green-function method" [16–20], which was developed about ten years ago and was successfully applied to many defects in semiconductors. The main limitation of this "defect-Green-function method" is that the real part of the Green function is evaluated from an energy integral over the imaginary part. Because a restriction to a finite energy range was necessary, the real part of the Green function was not very accurate. This did not cause problems in the description of sp-bonded defects but it prevented an accurate description of transition metals. Alternative formalisms, which allowed to deal with the latter systems have been developed by Dederichs, Zeller et al. [21, 22], by Gunnarsson et al. [23] and Beeler et al. [24]. Also, the approach of our self-consistent surface-Green-function (SSGF) method described below does not suffer from this problem. Besides, taking some ideas from the "defect-Green-function method" the new SSGF method is based on the layer-KKR Green-function formalism of Kambe, Scheffler and Máca [25, 26], combining it with ab-initio pseudopotential theory [27–30].

The remaining paper is organized as follows: section 2 outlines the key ideas of our method. We briefly indicate how these ideas are implemented in the numerical programs and we summarize the advantages and possible problems of the method. In section 3, we then present results for the electronic structures of two adsorbate systems, namely a single S adatom on Pd(1 0 0) and a single Na adatom on Al(1 0 0). With the discussion of the latter system, we contribute to a recent controversy concerning the question whether the adsorption of alkalis is ionic – as it was hitherto generally assumed [31] – or not – as it was argued recently in several publications [32–35]. In section 4, we give a summary.

2. Method

State-of-the-art self-consistent calculations face the problem to solve the Kohn–Sham equation

$$H\psi_i = E_i\psi_i \tag{1}$$

with

$$H = -\frac{\hbar^2}{2m}\nabla^2 + V_{\text{eff}}[n_v, r]\,, \tag{2}$$

where the effective potential functional is given by

$$V_{\text{eff}}[n_v, r] = V_{\text{ext}}(r) + e^2\int \frac{n_v(r')}{|r-r'|}\,\mathrm{d}^3r' + V_{\text{xc}}[n_v, r]\,. \tag{3}$$

V_{ext} is the external potential of the atomic nuclei or frozen-core ions. We will assume throughout this article that V_{ext} is given by ionic, ab-initio pseudopotentials [27–30], and $n_v(r)$ is then the density of the valence states. The density of the core electrons, $n_c(r)$, is kept frozen to the free atom density. Because $n_c(r)$ does not change, it is not noted in V_{ext} or in V_{xc} although it enters both.

For low-symmetry, poly-atomic ($\sim 10^{23}$ particles) systems the direct evaluation of eq. (1) is practically impossible. Therefore, one usually restricts investigations to periodic structures, where Bloch's theorem can be applied which reduces the size of the problem to a tractable one. Localized perturbations in macroscopic systems can only be approximately described by this procedure by introducing so-called "super-cells". The alternative approach which does not introduce an artificial periodicity is a Green-function method. Here the Hamiltonian of eqs. (2) and (3) is split into two parts,

$$H = H^0 + \Delta V\,, \tag{4}$$

where H^0 is an – in principle – arbitrary Hamiltonian ($H^0 = -(\hbar^2/2m)\,\Delta^2 + V^0$) and ΔV is the remainder. For our studies we take H^0 as the Hamiltonian of a semi-infinite crystal, described by muffin-tin potentials, and a simple surface barrier. For reasons which will become clear below, we take the muffin-tin potentials from self-consistent bulk calculations. For H^0 we have the two-dimensional Bloch theorem and its electronic structure can be calculated using the method of Kambe and Scheffler [25] and the published computer programs [26]. This gives the Green function

$$G^0(Z) = (Z - H^0)^{-1}\,, \tag{5}$$

with $Z = E + \mathrm{i}\eta$ in a high numerical accuracy. $G^0(Z)$ can be obtained for any energy on the real axis ($\eta \to +0$) or in the complex energy plane ($\eta > 0$). We like to emphasize that the real and imaginary parts of G^0 are obtained directly and simultaneously without carrying out a numerical Hilbert transformation. This is a significant difference to a predecessor of the present approach, the "defect-Green-function method" [16–20], and allows to treat simple metals as well as transition metals.

From $G^0(Z, r, r')$ we obtain the reference-system electron density

$$n^0(r) = -\frac{2}{\pi}\,\mathrm{Im}\int_{-\infty}^{E_F} G^0(Z, r, r')\,\mathrm{d}Z\,, \tag{6}$$

where E_F is the Fermi energy. It is determined by the bulk properties of V^0. Therefore it is important that V^0 takes the form of the self-consistent bulk potential. It is also important that the surface-barrier height together with E_F gives the correct work function of the clean surface. On the other hand, it is usually not necessary that V^0 is a correct, self-consistent surface potential, because the surface region, including muffin-tin corrections, will be evaluated in the next step.

Having obtained the Green function of the "clean surface", $G^0(Z)$, we can evaluate the Green function of the adsorbate system, written in operator form

$$G(Z) = (Z - H)^{-1}\,, \tag{7}$$

by solving

$$\Delta G(Z) = G(Z) - G^0(Z) = G^0(Z)\,\Delta V\,G(Z) = G^0(Z)\,\Delta V[1 - G^0(Z)\,\Delta V]^{-1}G^0(Z)\,. \tag{8}$$

As we have mentioned, it is not necessary that V^0, $G^0(Z)$ and $n^0(r)$ are self-consistent. However, eq. (8) should be evaluated in a self-consistent way using

$$\Delta V = V_{\text{eff}}[n_\nu] - V^0 , \tag{9}$$

where $V_{\text{eff}}[n_\nu]$ is given by eq. (13), and

$$n_\nu(r) = n^0(r) + \Delta n(r) , \tag{10}$$

with

$$\Delta n(r) = -\frac{2}{\pi} \operatorname{Im} \int_{-\infty}^{E_F} \Delta G(Z, r, r')\, dZ . \tag{11}$$

Equation (8) is an operator equation. So far, we have not introduced a basis set, but this will be done now. The basis set only needs to cover the real space within which $\Delta n(r)$ is localized. We will denote this region as A and the remaining region as B. Because crystals, and in particular metals, tend to screen perturbations, region A is usually very small. For a point defect in silicon and for adsorbates on metals the radius of this region is about 1–3 interatomic distances. In this region the basis set (which will be assumed to be orthonormal) should have sufficient flexibility to represent a sufficiently wide class of physically meaningful, localized functions $\Delta n(r)$,

$$\Delta n(r) = \sum_{i,j}^{\epsilon A} \Delta n_{ij}\, \chi_i(r) \chi_j^*(r) , \tag{12}$$

where Δn_{ij} are real numbers and $\Delta n_{ij} = \Delta n_{ji}$. Thus, we split the complete Hilbert space of H into two parts $\{\chi_i\}_A \oplus \{\chi_i\}_B$. The basis functions $\{\chi_i\}_A$ cover the spatial region A and are needed to represent the possible functions $\Delta n(r)$.

When such a basis set is introduced, the matrix of the potential pertubation takes the form

$$\Delta V = \begin{pmatrix} \Delta V_{AA} & 0 \\ 0 & 0 \end{pmatrix} . \tag{13}$$

To be precise, we will assume that $\|\Delta V_{AA}\| \gg \|\Delta V_{IJ}\|$ with (I, J) equal to (A, B), (B, A) or (B, B). Note that the real-space representation of ΔV is derived from eqs. (3), (9) and (10) and that it enters the calculations as an intermediate quantity which we have to project on the basis $\{\chi_i\}_A$.

Equation (8) now takes the form

$$\Delta G = \begin{pmatrix} \Delta G_{AA} & \Delta G_{AB} \\ \Delta G_{BA} & \Delta G_{BB} \end{pmatrix} , \tag{14}$$

with

$$\Delta G_{AA}(Z) = G^0_{AA}\, \Delta V_{AA} \times [1_A - G^0_{AA}(Z)\, \Delta V_{AA}]^{-1} G^0_{AA}(Z) . \tag{15}$$

And the matrix Δn_{ij} of eq. (12) is given by

$$\Delta n_{ij} = -\frac{2}{\pi} \operatorname{Im} \int_{-\infty}^{E_F} \Delta G_{ij}(Z)\, dZ . \tag{16}$$

The change in the total density of states is

$$\Delta N(Z) = -\frac{2}{\pi} \sum_{i}^{\epsilon A \oplus B} \operatorname{Im} \Delta G_{ii}(Z) = \frac{2}{\pi} \frac{d}{dZ} \delta(Z) , \tag{17}$$

with the generalized phase shift [36]

$$\delta(Z) = -\operatorname{Im} \ln \det[1 - G^0(Z)\, \Delta V] = -\operatorname{Im} \ln \det[1_A - G^0_{AA}(Z)\, \Delta V_{AA}] . \tag{18}$$

$\Delta N(Z)$ will usually differ from the local density of states change (compare fig. 2 below),

$$\Delta N^{\text{local}}(Z) = -\frac{2}{\pi} \sum_{i}^{\epsilon A} \operatorname{Im} \Delta G_{ii}(Z) . \tag{19}$$

Although the two functions given by eqs. (17) and (19) are usually different, the integrals should be the same

$$\int_{-\infty}^{E_F} \Delta N^{\text{local}}(Z)\, dZ = \int_{-\infty}^{E_F} \Delta N(Z)\, dZ = \int \Delta n(r)\, d^3r = \sum_{i}^{\epsilon A} \Delta n_{ii} = -Z_\nu . \tag{20}$$

This is an important condition which guarantees that the system stays neutral. Z_v is the valency of the adsorbate, i.e. of ΔV_{ext}. Equation (20) is also an important (but still not sufficient) test if the basis set $\{\chi_i\}_A$ is appropriate.

The approach described above corresponds to the Green-function *operator* method. Note that all important quantities, like the local density of states (eq. (19)), the total density of states (eqs. (17), (18)), and the electron density change (eqs. (12), (16), (17)) are only determined by the region A. Experience for defects in the bulk of crystals has shown [19, 24] that only a rather small set of basis functions is required in order to fulfill eqs. (12) and (13). Our (still limited) experience with the new SSGF method indicates that this is also true for surfaces. As an example we show in fig. 1 the electron density calculated for Na on Al(1 0 0); the physics of this system will be discussed in section 3.2 below. The reference system is built from a self-consistent aluminum bulk calculation. The surface is simulated by a simple step function the height of which is obtained from the theoretical Fermi energy and the experimental work function $\Phi_{Al(100)} = 4.4\,eV$ [37]. For the self-consistent

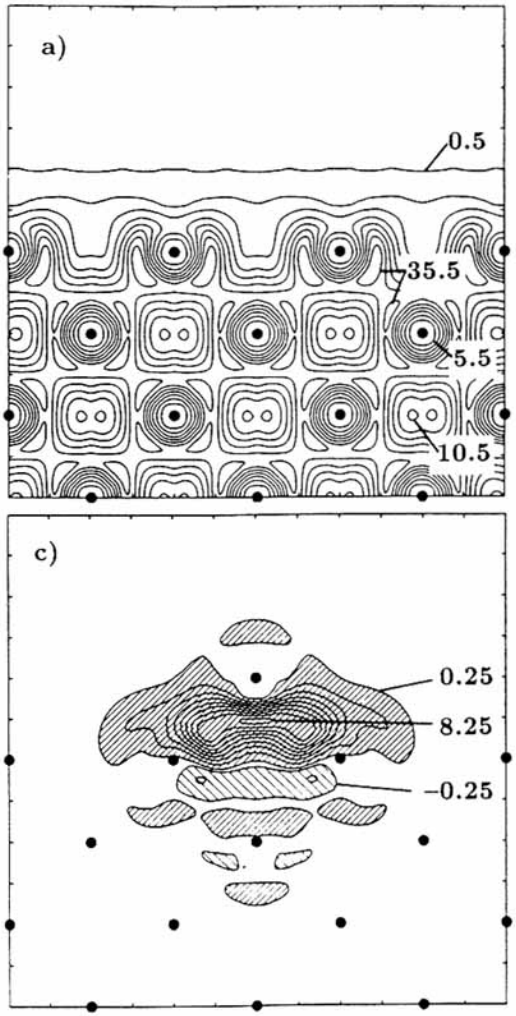

Fig. 1. Electron density for (a) the clean Al(1 0 0) surface, (b) the adsorbate system of a single Na atom on Al(1 0 0), and (c) the adsorbate induced density change (i.e. the difference of figs. (b) and (a)). Units are 10^{-3} bohr^{-3}. The step between contour lines is 5×10^{-3} bohr^{-3} in figures (a) and (b). In figure (c) the separation between contours is 1×10^{-3} bohr^{-3}. Densely hatched areas indicate an accumulation of electron density (positive $\Delta n(r)$). Sparsely hatched areas correspond to an electron depletion (negative $\Delta n(r)$). Positions of nuclei are marked by dots.

Green-function calculation we then used s, p and d functions centered at the adsorbate and at its five Al neighbors. We used Gaussians with three decays (0.25, 0.50 and 1.00 bohr^{-2}). This gives a total of 162 basis functions which we find to be sufficient to obtain a converged $\Delta n(\boldsymbol{r})$. In fact, the function $\Delta n(\boldsymbol{r})$ oscillates (see fig. 1(c)), but is sufficiently simple to be described in terms of eq. (12).

We conclude this section by summarizing the main advantages of the SSGF method.

1. The method avoids to calculate wave functions.
2. The Green-function approach enables to use a rather small and simple basis set: We only have to represent one function, $\Delta n(\boldsymbol{r})$, which is very localized and usually not very complicated. $\Delta n(\boldsymbol{r})$ then refines the change in the potential, which has to be projected on the basis. We do not have to represent the full Hamiltonian.
3. In the Green-function *operator* approach the perturbation is only due to the potential difference, ΔV. This is usually a well localized function. In contrast to the *matrix* Green-function method [13–15], we do not get a perturbation contribution from the kinetic energy which would have a somewhat longer range.
4. Last but not least we mention that the method is computationally very efficient, if compared to other self-consistent surface methods. For the calculations of an adsorbed atom (compare section 3.2 below) we need about four hours of CPU time on a CONVEX C2 computer to set up the clean-surface Green function and another 3–5 hours for the self-consistent calculation of the adsorbate's Dyson equation. Note that the Green function $G^0(Z)$ has only to be calculated once and is independent from the adsorbate atom and its position. Thus, the method is in particular suited for trend studies investigating many different adsorbate atoms.

We should also mention the possible disadvantages of our approach.

1. The definition of the basis set is not very precise (see the discussion of eqs. (12) and (13)). We note, however, that we have not found any severe problems with this point so far.
2. Using a potential for V^0 which is self-consistent in the bulk, but not at the clean surface, makes the calculation of $G^0(Z)$ very efficient. In the self-consistent calculations for the adsorbate, V^0 will be only corrected locally, i.e. in the region of the adparticle. Whether or not this is sufficient will show up in the calculations, but one should be aware of possible problems.
3. Although the operator $G^0(Z, \boldsymbol{r}, \boldsymbol{r}')$ is calculated very accurately, its projection onto the localized basis set is at present performed by approximating the crystal volume by a sum over overlapping atom-centered spheres [38]. This simplifies the calculation of the matrix $G^0_{AA}(Z)$, but it implies that the interstitial region is not described very accurately. We believe that for close-packed structures this is not a severe approximation.

3. Applications

Several test calculations have been performed using the method described above. These tests are described elsewhere. Below we give two examples for adsorbates to show the rapid convergence of results with the basis set (section 3.1) and to address a recent question concerning the low coverage limit of alkali adsorption on metals (section 3.2).

3.1. *An isolated S atom on Pd(1 0 0)*

The main purpose of this section is to demonstrate the efficiency of our method and to explain the differences of local and total densities of states (see eqs. (17) and (19)). We discuss electronic-structure calculations for S adsorbed on Pd(1 0 0). The S atom is positioned at the fourfold hollow site with a S–Pd bond length of 2.78 Å, which equals the Pd–Pd bond length. This bond length was chosen for convenience. It is larger than the S–Pd bond length as de-

termined for a periodic S layer on Pd(1 0 0) [39] which has a S–Pd distance of 2.35 Å. The S potential is taken from a neutral free atom pseudopotential [38]. Although these Green-function calculations are not self-consistent and also the geometry is not optimized they are well suited for the purpose of this section. We also note that the calculated density of states is already (to some extent) physically meaningful. This is due to the fact that $\Delta N(E)$ is largely determined by the clean-surface density of the states: As it can be inferred from eq. (18) [19], minima in Tr Im $G^0_{AA}(E)$ will often give rise to resonances in $\Delta N(E)$. These resonances are not very sensitive to the potential ΔV.

Figure 2 compares our results for the local and total densities of states using a single-center basis centered at the adsorbate and a five-center basis. We use s, p and d Gaussians and three decays (0.3, 0.5 and 1.7 bohr^{-2}). It is intriguing that $\Delta N(E)$ is already described very well, when only a single-center basis (27 orbitals) is used (compare figs. 2(b) and 2(d)). On the other hand we see that the local density of states, $\Delta N^{\text{local}}(E)$, exhibits the main peaks which are also found in $\Delta N(E)$, but otherwise it is clearly different. Even the five-center basis $\Delta N^{\text{local}}(E)$ clearly differs from $\Delta N(E)$. In fact, a much larger basis set would be required to achieve that both functions agree, but in general there is no reason why such an attempt should be made. It is worth noting that an inspection of $\Delta N^{\text{local}}(E)$ may usually be helpful, as it indicates at which energies new states appear which have a reasonable amplitude in the region of the adsorbate. This may have a closer relation to adsorbate chemistry than struc-

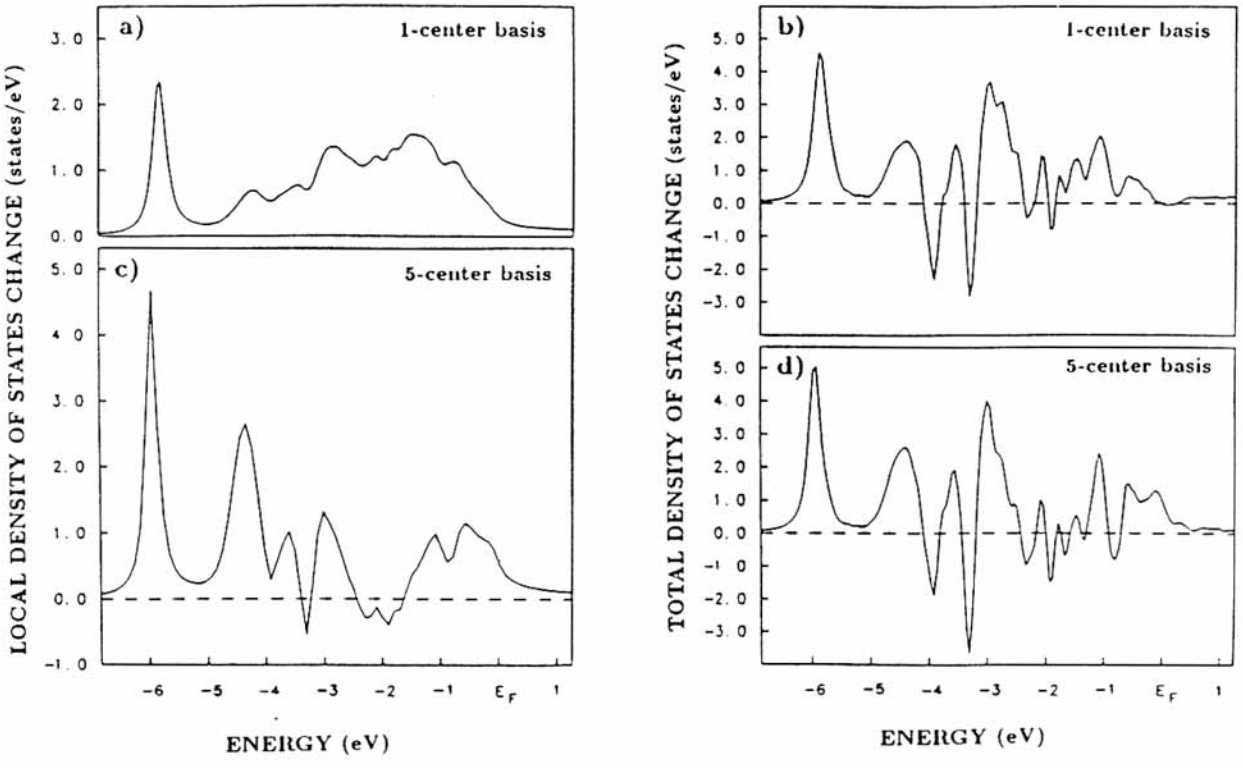

Fig. 2. Local density of states changes (left) and total density of states changes (right) for the S adsorbate on Pd(1 0 0). Figures (a) and (b) show the results of a single-center basis calculation (27 basis functions) and figures (c) and (d) correspond to a five-center basis (135 basis functions).

tures in $\Delta N(E)$ which are in part due to very extended wave functions.

The wave function analysis of the calculations of fig. 2 shows [38] that the sulfur p_z orbital forms a covalent bond with the substrate and gives rise to the peak in the density of states at about 6 eV below the Fermi energy. This peak is very sharp, because it is shifted below the Pd density of states. The sulfur p_x, p_y orbitals, which are oriented parallel to the surface, interact less strongly with the Pd states. They give rise to some resonance structures (see fig. 2(d)) as for example that at 4.5 eV below E_F, which is just at the lower edge of the Pd d band. In the range above $E_F - 4.5$ eV we find a complicated resonance and antiresonance structure. Both, the p_z and p_x, p_y-like state, have a resonance at $E_F - 3$ eV (fig. 2(d)) which is pinned at this energy by a dip in the density of states of the clean Pd surface.

3.2. An isolated Na atom on Al(1 0 0)

The interaction of a single alkali atom with a perfect-crystal metal surface represents probably the most simple chemisorption system. Nevertheless, over the last years it became clear from several experimental and theoretical studies [32–35] that it is a matter of high controversy what are the dominant quantum-mechanical interactions in this system. Whereas the Langmuir–Gurney model [40–42], which invokes a partial charge transfer from the alkali atom to the metal substrate, had been accepted for many decades, it was concluded from recent ab-initio calculations [32, 35] and experimental studies [33, 34] that the alkali atom adsorbed on metals is bonded with practically zero charge transfer. The reason for this controversy is largely due to the fact that parameter-free, self-consistent calculations describing the alkali adsorption on realistic (atomistic) metal surfaces only exist for thin metal slabs (simulating the substrate) and periodic adlayers [32, 35]. For the low coverage limit ($\Theta \rightarrow 0$) such calculation were lacking so far.

The calculations are performed using ab-initio pseudopotentials for the ions [29]. Tests of the quality of the basis set have been performed to ensure that the results reported below are well converged [43]. These results are obtained with s, p and d Gaussians with three decays (0.25, 0.50 and 1.00 bohr^{-2}) centered at the adsorbate, at its four top-layer Al neighbors, and at the Al atom below it, in the second Al layer. Details of these calculations will be published elsewhere.

Some results were shown in fig. 1 above. Figure 3 shows the self-consistent change of the electron density:

$$n^{\Delta} = n^{\mathrm{Na/Al(100)}} - n^{\mathrm{Na}} - n^{\mathrm{Al(100)}} . \qquad (21)$$

Here, $n^{\mathrm{Na/Al(100)}}$ is the self-consistent electron density of the adsorbate system Na on Al(1 0 0) (see fig. 1(b)). n^{Na} is the electron density of the free, neutral Na atom, and $n^{\mathrm{Al(100)}}$ is the density of the references system, namely the semi-infinite Al(1 0 0) surface (see fig. 1(a)). Figure 3 reveals that the electron-density change is very localized. We see that, compared to the free,

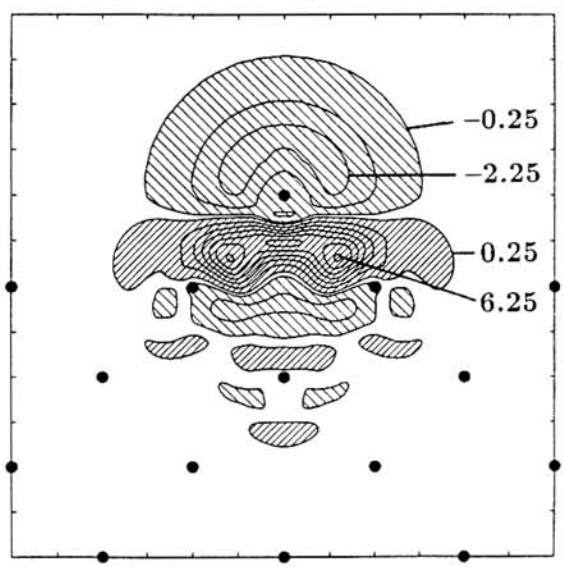

Fig. 3. Electron-density change, $n^{\Delta}(r)$, for Na adsorbed on Al(1 0 0). For the definition of n^{Δ} see eq. (21); n^{Na} is taken from a free, neutral atom. Units are 10^{-3} bohr^{-3}. The step between contour lines is 1×10^{-3} bohr^{-3}. Densely hatched areas indicate accumulation of electron density (positive $n^{\Delta}(r)$). Sparsely hatched areas correspond to electron depletion (negative $n^{\Delta}(r)$). The positions of nuclei are marked by dots.

neutral atom, the adsorbed atom has lost charge on the vacuum side while there is an accumulation of charge on the metal side. Our results, which fully include the atomic structure of the substrate, are qualitatively similar to n^{λ} obtained by Lang and Williams [44] in their study of Li adsorbed on jellium. Important information, which is not contained in the Li/jellium results, is the behavior relative to the nuclei of the substrate. We see that the adsorbate-induced change of the electron density (fig. 1(c)) oscillates, having nodes at the substrate nuclei. From figs. 1(c) and 3 it is not clear whether these results should be interpreted in terms of an internal polarization of the adatom, i.e. a hybridization of the Na 3s and $3p_z$ orbitals, or in terms of charge transfer. The similarity between these two possibilities would also complicate an interpretation of experimental results which try to probe $\Delta n(\boldsymbol{r})$ (i.e. fig. 1(c)). In fact, one could safely argue that a clear distinction between the polarization and charge-transfer pictures is not possible.

A further analysis of our calculations shows that the picture of a partially ionized alkali atom is indeed appropriate. For a neutral Na atom far away from the Al(1 0 0) surface the DFT-LDA eigenvalue E_{3s}^{Na} is above the metal Fermi level at -2.82 eV below vacuum. The calculated ionisation energy, as obtained from the transition state, is 5.21 eV, which agrees well with the experimental result of 5.14 eV. Our calculations also give, that the distant alkali atom, when brought in equilibrium with the Al(1 0 0) Fermi level, will partially ionize to an occupation $n_{3s} = 0.65$. Thus, 0.35 electrons are transferred to the metal. The now slightly positively charged alkali atom induces an image charge density in the metal surface. Figure 3 shows that this picture remains *qualitatively* valid when the alkali approaches the surface and adsorbes. The upper half of the adsorbed Na has a negative n^{λ} and thus a smaller electron density than the free, neutral alkali atom.

In order to elaborate on this "charge transfer picture" we show in fig. 4(a) plots of $n^{\lambda}(n_{3s} = 0.1)$, where n^{Na} (compare eq. (21)) is now taken from a self-consistent calculation for the partially ionized free atom. This picture describes the response of the Na–Al (1 0 0) system to the partially ionized Na atom. In order to determine whether this figure should be interpreted in terms of a hybridization of Na s and p_z states (internal polarization), in terms of covalent bonding between the Na atom and the substrate, or in terms of metallic screening, we compare it to a result of a calculation which only contains the metallic screening (fig. 4(b)). Figure 4(b)

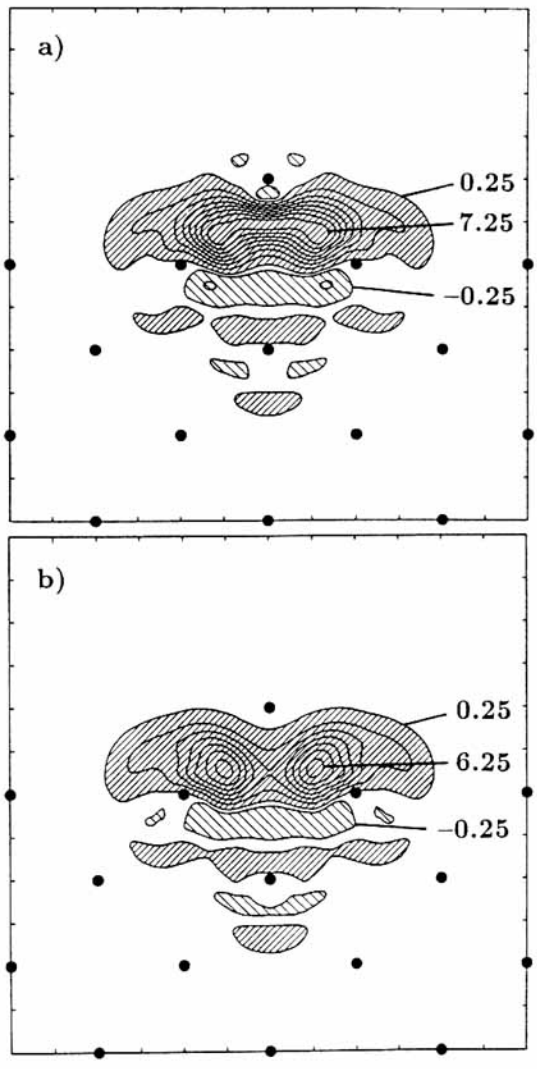

Fig. 4. Same as fig. 3 but in part (a) we now take for n^{Na} the partially ionized free Na atom. Units are 10^{-3} bohr^{-3}. Part (b) shows the screening charge density of an external point charge of $-0.1\,e$. Here the units are 10^{-4} bohr^{-3}.

displays the screening charge density which we obtain for an external point charge (see fig. 4(b)). The shape of this screening charge density is very similar for a negative point charge and for a positive point charge, as long as the latter is sufficiently weak, so that it cannot bind an electron. The magnitude of the contour lines nearly scale linearly with the magnitude of the external point charge [43]. The similarity between figs. 4(a) and (b) is quite surprising, because a Na-ion is – of course – different from a point charge. Nevertheless, the response of the metal is similar for both cases. The slight differences between figs. 4(a) and (b) may be interpreted as an indication that some covalency and some s–p_z mixing are present in the Na–Al(1 0 0) interaction, but that these contributions are not very large. From the similarity of figs. 4(a) and (b) we conclude that the "charge transfer picture" is indeed useful and appropriate to describe the physics of alkali adsorption at low coverage. However, charge transfer alone is not sufficient to understand the resulting $\Delta n(r)$. It is important to realize that the charge transfer actuates a significant change in the surface electron density. Because the metal screening charge is largely located in front of the metal (see fig. 4(b)), the adsorbate induced electron-density change (see fig. 1(c)) cannot be divided any more directly into adsorbate and metal contributions. As a consequence of this difficulty one may be tempted to abandon the charge transfer picture for this adsorbate system. We believe, however, that one would then give up an important piece of physical understanding.

For higher coverage adlayers or for adsorbate islands the picture discussed above will change, because then the Na 3s orbitals will interact and form a band.

4. Summary

In this paper we described the key ideas of a recently developed Green-function approach, which allows to treat a localized perturbation on the surface of a semi-infinite crystal. By this method theoretical studies of the initial stage of adsorption ($\Theta \to 0$) become feasible. No shape approximations to the potential and the charge density are applied in the region of the adparticle; only further away from this region the potential is approximated by the muffin-tin form. The method is extremely efficient, compared to other self-consistent surface methods, and it is in particular suited for trend studies, investigating different adatoms. We presented results of investigations of a single Na atom adsorbed on Al(1 0 0). These calculations show that the "charge transfer picture" of alkali adsorption on metals is indeed a useful concept. It is, however, important to realize that the charge transfer is followed by a screening-charge density in the metal. Both effects together give rise to the adsorbate induced electron density shown in fig. 1(c). Some covalent contribution to the bonding is also present, but this is quite small.

Acknowledgement

Discussions with J. Bormet and K. Kambe are gratefully acknowledged.

References

[1] N.H. March and S. Lundqvist, eds., The Inhomogeneous Electron Gas (Plenum, New York, 1984).
[2] M.L. Cohen, in: Highlights of Condensed-Matter Theory, eds. F. Bassani, F. Fumi and M.P. Tosi (North-Holland, Amsterdam, 1985) p. 16.
[3] O.K. Andersen, O. Jepsen and D. Glötzel, in: Highlights of Condensed-Matter Theory, eds. F. Bassani, F. Fumi and M.P. Tosi (North-Holland, Amsterdam, 1985) p. 59.
[4] K.P. Bohnen and K.M. Ho, Vacuum 41 (1990) 416.
[5] F. Manghi, R. Del Sole, A. Selloni and E. Molinari, Phys. Rev. B 41 (1990) 9935.
[6] M. Weinert, E. Wimmer and A.J. Freeman, Phys. Rev. B 26 (1982) 4571.
[7] E. Wimmer, H. Krakauer, M. Weinert and A.J. Freeman, Phys. Rev. B 24 (1981) 864.
[8] P. Krüger and J. Pollmann, Phys. Rev. Lett. 64 (1990) 1808.
[9] P. Krüger and J. Pollman, Phys. Rev. B 38 (1988) 10578.
[10] G.A. Benesh and J.E. Inglesfield, J. Phys. C 17 (1984) 1595.

[11] G.C. Aers and J.E. Inglesfield, Surf. Sci. 217 (1989) 367.
[12] J.E. Inglesfield and G.A. Benesh, Phys. Rev. B 37 (1988) 6682.
[13] A.R. Williams, P.J. Feibelman and N.D. Lang, Phys. Rev. B 26 (1982) 5433.
[14] P.J. Feibelman, Phys. Rev. B 35 (1987) 2626.
[15] P.J. Feibelman, Phys. Rev. Lett. 65 (1990) 729.
[16] J. Bernholc, N.O. Lipari and S.T. Pantelides, Phys. Rev. Lett. 41 (1978) 895; Phys. Rev. B 21 (1980) 3545.
[17] G.A. Baraff and M. Schlüter, Phys. Rev. Lett. 41 (1978) 892; Phys. Rev. B 19 (1979) 4965.
[18] G.A. Baraff, E.O. Kane and M. Schlüter, Phys. Rev. B 21 (1980) 5662.
[19] M. Scheffler, in: Festkörperprobleme XXII, ed. P. Grosse (Vieweg, Braunschweig, 1982) p. 115.
[20] M. Scheffler, J.P. Vigneron and G.B. Bachelet, Phys. Rev. Lett. 49 (1982) 1765; Phys. Rev. B 31 (1985) 6541.
[21] P.J. Braspenning, R. Zeller, A. Lodder and P.H. Dederichs, Phys. Rev. B 29 (1984) 730.
[22] B. Drittler, M. Weinert, R. Zeller and P.H. Dederichs, Phys. Rev. B 39 (1989) 930.
[23] O. Gunnarsson, O. Jepsen and O.K. Andersen, Phys. Rev. B 27 (1983) 7144.
[24] F. Beeler, O.K. Andersen and M. Scheffler, Phys. Rev. Lett. 55 (1985) 1498; Phys. Rev. B 41 (1990) 1603.
[25] K. Kambe and M. Scheffler, Surf. Sci. 89 (1979) 262.
[26] F. Máca and M. Scheffler, Comp. Phys. Commun. 38 (1985) 403; 47 (1987) 349; 51 (1988) 381.
[27] D.R. Hamann, M. Schlüter and C. Chiang, Phys. Rev. Lett. 43 (1979) 1494.
[28] G. Kerker, J. Phys. C 13 (1980) L189.
[29] G.B. Bachelet, D.R. Hamann and M. Schlüter, Phys. Rev. B 26 (1982) 4199.
[30] R. Stumpf, X. Gonze and M. Scheffler, A list of separable norm-conserving, ab-initio pseudopotentials, Fritz-Haber-Institut, Research Report (April 1990).
[31] H.P. Bonzel, A.M. Bradshaw, and G. Ertl, eds., Physics and Chemistry of Alkali Metal Adsorption (Materials Science Monograph 57) (Elsevier, Amsterdam, 1989).
[32] H. Ishida and K. Terakura, Phys. Rev. B 38 (1988) 5752.
[33] M.-L. Shek, J. Hrbek, T.K. Sham and G.-Q. Xu, Phys. Rev. B 41 (1990) 3447.
[34] D.M. Riffe, G.K. Wertheim and P.H. Citrin, Phys. Rev. Lett. 64 (1990) 571.
[35] E. Wimmer, A.J. Freeman, M. Weinert, H. Krakauer, J.R. Hiskes and A.M. Karo, Phys. Rev. Lett. 48 (1982) 1128.
[36] Essential elements of the Green-function formalism are described in the paper by G.F. Koster and J.C. Slater, Phys. Rev. 94 (1954) 1392; 95 (1954) 1165, and J. Callaway, J. Math. Phys. 5 (1964) 783; Phys. Rev. 134 (1967) 515.
[37] J.K. Grepstadt, P.O. Gartland and B.J. Slagsvold, Surf. Sci. 57 (1976) 348.
[38] Ch. Droste, Ph.D thesis, Technische Universität Berlin (1990).
[39] W. Berndt, R. Hora and M. Scheffler, Surf. Sci. 117 (1982) 188.
[40] J.B. Taylor and I. Langmuir, Phys. Rev. 44 (1933) 423.
[41] R.W. Gurney, Phys. Rev. 47 (1934) 479.
[42] J.P. Muscat and D.M. Newns, Surf. Sci. 84 (1979) 262.
[43] G. Barzel and M. Scheffler, unpublished.
[44] N.D. Lang and A.R. Williams, Phys. Rev. B 16 (1977) 2408; 18 (1978) 615.